Parmelee, H. M., "Water Solubility of 'Freon' Refrigerants," *Refrig. Eng.* (Dec., 1953).
Pigford, R. L., and C. Pyle, "Performance Characteristics of Spray-Type Adsorption Equipment," *Ind. Eng. Chem.*, 43, 1649 (1951).
Ross, T. K., and H. J. Coombe, "Gas Absorption in a Multiple Liquid-Jet Contactor," *Trans. Inst. Chem. Engrs.*, 44, T160 (1966).
Ruckenstein, E., "Mass Transfer Between a Single Drop and a Continuous Phase," *Intern. J. Heat Mass Trans.*, 10, 1785 (1967).
Stirba, C., and D. M. Hurt, "Turbulence in Falling Liquid Films," *AIChE J.*, 1, 178 (1955).
Wilke, C. R., and P. Chang, "Correlation of Diffusion Coefficients in Dilute Solutions," *ibid.*, 264 (1955).
Witherspoon, D. A., and L. Bonoli, "Correlation of Diffusion Coefficients for Paraffin, Aromatic, and Cycloparaffin Hydrocarbons in Water," *Ind. Eng. Chem. Fundamentals*, 8, 589 (1969).

Manuscript received October 1, 1976; revision received January 24, and accepted February 1, 1977.

Photoassisted Heterogeneous Catalysis with Optical Fibers:

I. Isolated Single Fiber

RICHARD E. MARINANGELI
and
DAVID F. OLLIS

Department of Chemical Engineering
Princeton University
Princeton, New Jersey 08540

Recently reported varieties of photoassisted heterogeneous catalysts are summarized. A cylindrical, light carrying, optical fiber coated with a catalyst layer is evaluated as a novel configuration for all such light assisted catalysis. Equations are obtained which describe the light intensity in the fiber and its surrounding catalyst layer. A dimensionless group of the form $\Phi = (4\alpha_c\beta_c dL)/(d_f)$ [$d = d_c$ for $d_c < \lambda$, $d = 0(\lambda)$ for $d_c > \lambda$] determines the relative influence of light loss by all absorption and scattering to light transported in the fiber length. An effectiveness factor η_I for heterogeneous photoassisted catalysis is determined for reactions which are first order in intensity and without mass transport limitations. Asymptotic forms of η_I are $\eta_I = 1.0$ ($\Phi << 1.0$) and $\eta_I = \Phi^{-1}$ ($\Phi >> 1.0$).

SCOPE

Heterogeneously catalyzed photoassisted reactions occur at ambient temperature and low pressures. If the corresponding present or future photoassisted heterogeneous catalysts are to be useful, scale-up configurations which contain both high surface areas per volume and convenient light-distribution to the catalyst phase must be developed. One such general configuration, conceptually applicable to all such reported catalysts, is an optical fiber which is coated with a layer of the photo-utilizing catalyst. The present paper evaluates the change in light intensity as a light beam, entering the fiber end, is repeatedly internally reflected down the fiber length, contacting the catalyst coating at each reflection. The principles of fiber optics and Internal Reflection Spectroscopy determine which factors influence the transport of light in the presence of scattering and absorption. A review of the extant photoassisted catalysts indicates that the analysis should include thin ($d_c << \lambda$), thick ($d_c >> \lambda$), and intermediate catalyst films. In all cases, an effectiveness factor for light transport is defined and evaluated, its asymptotic forms being the same as are well known for mass diffusion, even though the appropriate equations are first rather than second order. Assembly of such fibers into a macroscopic bundle is considered in a subsequent paper (Marinangeli and Ollis, 1977).

CONCLUSIONS AND SIGNIFICANCE

For thin, thick, or intermediate thickness concentric catalyst coatings, an equation of the form $d\psi/d\xi + \Phi\psi = 0$ determines the axial profile of light intensity ψ with axial distance ξ in the optical fiber. Thus, the appropriately defined effectiveness factor for light transport depends on the single dimensionless group Φ which is a function of fiber length, fiber diameter, catalyst film thickness, catalyst absorption, and illumination wavelength. The single fiber effectiveness factor offers a means for correlating experimental data obtained from single, optical, fiber-catalyst systems. Effectiveness factors for macroscopic (multifiber) configurations including simultaneous influences of light, heat, and mass transfer are reported in a subsequent paper.

Correspondence concerning this paper should be addressed to David F. Ollis.

A photoassisted heterogeneously catalyzed reaction is a reaction for which a photon excitable catalyst site is in or on a phase distinct from that which supplies the reactant(s). The photoexcitation step typically involves energies on the order of a few electron volts (for example, 400 nm = 3.1 eV), corresponding to promotions such as semiconductor band gap excitation or metal complex electronic transitions. At least one possible deexcitation route drives the catalyzed reaction step, hence the terminology photoassisted catalysis.

Noncatalyzed photochemistry is typified by energetic reaction intermediates (for example, free radicals) and by coupling of the momentum, mass, thermal energy, and radiant energy conservation equations, which make reactor design difficult (Cassano et al., 1967; Harano and Matsura, 1972). In contrast, catalyzed photochemical reactions appear to have relatively simple kinetics and high selectivity, suggesting intermediates of lesser reactivity. The rate typically is determined by the product of the quantum yield, the radiant intensity, and a function depending upon mass concentrations. The observed quantum yield may depend on the absorption coefficient of the catalyst. Since the catalyst concentration is constant, however, the absorption coefficient is constant for a given wavelength. Design of homogeneous photochemical reactors has received considerable attention, whereas analyses of catalyzed photochemical reactors have not yet been presented, except for certain photosynthetic reactors which are not similar to the coated light fiber

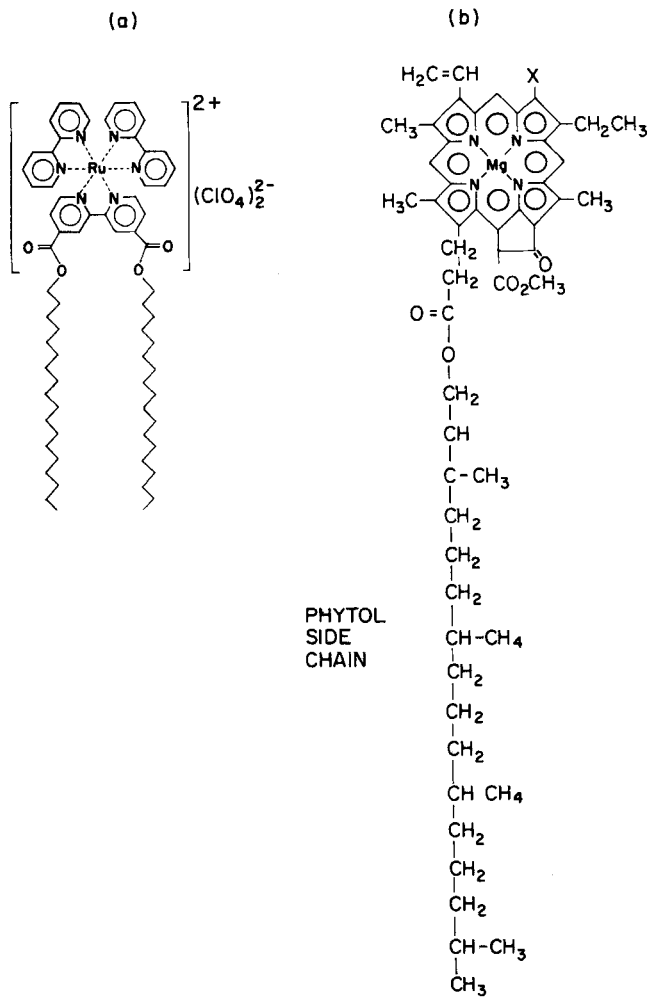

Fig. 1. (a). Structure: surfactant analog of tris (2,2′ bipyridine) ruthenium $(II)^{2+}$ prepared by replacement of a 2,2′-dioctadecyl ester. (b). Structure: chlorophyll (X-CH_3 [chlorophyll a]), (X-CHO [chlorophyll b]).

concept. In particular, the dimensionless groups which control the properties of noncatalyzed photochemical reactors have been elucidated (Dolan et al., 1969), and light intensity profiles for various reactors have been determined (Jacob and Dranoff, 1969; Matsuura and Smith, 1970; Jacob and Dranoff, 1970; Zolner and Williams, 1971; Irazoqui et al., 1973; Cerda et al., 1973; Roger and Villermaux, 1975). In view of the recent advances in photoassisted heterogeneous catalysts, suitable catalyst and reactor configurations for these newer catalysts are now logically considered. Heterogeneous photocatalysis in a slurry reactor has been examined by Hacker and Butt (1975); Laidler and Markham (1953), and others. The present paper considers a novel configuration which allows higher illuminated surface area per reactor volume than a slurry.

To establish reasonable catalyst dimensions for subsequent analysis, the various catalysts must be considered. The photoassisted electrolysis of water to hydrogen and oxygen has been reported by several groups (Fujishima and Honda, 1972; Wrighton et al., 1975; Hardee and Bard, 1975; Wrighton et al., 1976*a, b, c*; Ellis et al, 1976). Water may be electrolyzed in a cell if a potential of more than 1.26 V is applied. In principle, some or all of the potential required for electrolysis could be provided by photons if an illuminated semiconductor with a band gap of greater than 1.26 eV is used as one of the electrodes. While many such semiconductors are unstable during prolonged photoassisted electrolysis, titanium dioxide is stable and active provided an independent emf is applied simultaneously. Hence, a current is applied and electrical energy is consumed for each hydrogen molecule generated. Recent work has sought stable, active, photoassisted semiconductor electrodes which photolyze water without an applied emf. Crystals of $SrTiO_3$ (Wrighton et al., 1976*b*) and the perovskites $KTaO_3$ and $Kta_{0.77}Nb_{0.23}O_3$ (Ellis et al., 1976) satisfy the last restriction; the resulting current can be driven entirely by incident photons.

The heterogeneously catalyzed photooxidation of one to seven carbon alkanes has also been demonstrated convincingly. Excellent selectivity for the partial oxidation of alkanes to ketones and aldehydes can be obtained with illuminated titanium dioxide (Formenti et al., 1971, 1973, 1974; Djeghri et al., 1974). These reactions are highly exothermic, for example, for $i\text{-}C_4$ to acetone, $\Delta H_f = -962$ *kJ*/mole, but the activity of the catalyst decreases sharply at 110°C and drops to zero at 150°C (Formenti et al., 1971, 1974).

Reactions such as deuterium exchange and carbon monoxide oxidation (Murphy et al., 1976) have also been studied over illuminated semiconductors. In these experiments, the dependence of the catalytic activity on wavelength can elucidate the energy of electronic transitions involved in the catalysis. The principles of photoassisted catalysis, deduced from such experiments, have been reviewed (Wolkenstein, 1973; Freund and Gomes, 1969).

The heterogeneously catalyzed photoassisted cleavage of water by a surfactant complex of tris (2,2′-bipyridine) ruthenium $(II)^{2+}$ has been reported recently (Sprintschnik et al., 1976). The excited states of the original soluble ruthenium complex generally are not able to reduce water to hydrogen, since excited state decay of the soluble complexes is rapid. A stearate esterification of the soluble complex yields a surface active mixture which, in monolayer assemblies supported on glass, was reportedly capable of photoassisted cleavage of water to hydrogen and oxygen. The ruthenium complex appears

structurally and energetically related to the natural photo-assisted surface active catalysts, chlorophylls a and b, as seen from Figure 1. In each catalyst structure, a central metal ion is coordinated to the nitrogen atoms associated with heteroaromatic structures. These delocalized electron systems appear to be responsible for the initial capture of photons, that is, for the absorption spectrum of the catalyst.

A still more recent report from the same group (Sprintschnik et al., 1977) found that the purified form of the major ruthenium surfactant of the first study was *inactive*, these complexes clearly need further study.

The natural surfactants, chlorophylls *a* and *b*, have been immobilized on platinum electrodes; the co-immobilization, a redox compound (naphthoquinone or anthrahydraquinone) with the chlorophylls allowed operation of a photoelectrolysis cell (Takahashi and Kikuchi, 1976).

Photoassisted catalysts may become practically useful if a relatively cheap source of light with appropriate wavelength is available, the obvious source being the sun. Unfortunately, titanium dioxide has a band gap of about 3.0 eV; thus, alkane partial oxidation activity drops off sharply between 350 and 420 nm wavelengths (Formenti et al., 1971). As only a few percent of the solar spectrum lies below 350 nm, stable photoactive catalysts must be developed with smaller band gaps if utilization of a larger fraction of solar illumination is to be achieved. Practically, a semiconductor with a 1.4 eV band gap could be active for the photoassisted electrolysis or cleavage of water. Such a catalyst would use most of the solar spectrum. A catalyst with a band gap of 2.0 eV and a quantum yield of 0.5 could use more than 10% of the incident solar energy for the conversion of water into hydrogen and oxygen (Paleocrasses, 1974). Similar comments apply to surfactant metal complexes which are photo-catalysts. If such catalysts have absorption maxima in the visible, and if the catalytic action spectrum is the same as the absorption spectrum, as is true for chlorophyll, the surfactant catalyst could clearly utilize a larger fraction of the solar spectrum than the metal oxide semiconductors. (The direct solar spectrum peaks near 480 nm, dropping to zero at about 300 nm.)

Solar energy can be concentrated tenfold by stationary collectors (Rabl et al., 1974); higher concentrations require more expensive tracking systems. The use of artificial light sources could be justified, however, for the production of more valuable products than hydrogen or acetone. Both photoassisted catalysts and solar and artificial illumination are clearly available. The problem of development of suitable scale-up configurations remains.

THE CONCEPT: CATALYST COATED OPTICAL FIBERS

Scale-up of light consuming, heterogeneously catalyzed reactions must anticipate several problems concerning heat and mass transfer. Since the titanium dioxide oxidation catalyst is limited to 110° to 150°C, a similar temperature limit is likely to be present for the various semiconductor electrodes. Considerable concentration of illumination may overheat the surface, especially when an exothermic partial oxidation occurs, so the appropriate design must allow suitable temperature control. A monolayer of the ruthenium surfactant catalyst absorbs only about 1% of a light beam at normal incidence; a useful scale-up design must allow repeated contacting of catalyst with the unconsumed transmitted rays.

A configuration satisfying both requirements is an optical fiber coated with the appropriate photoassisted

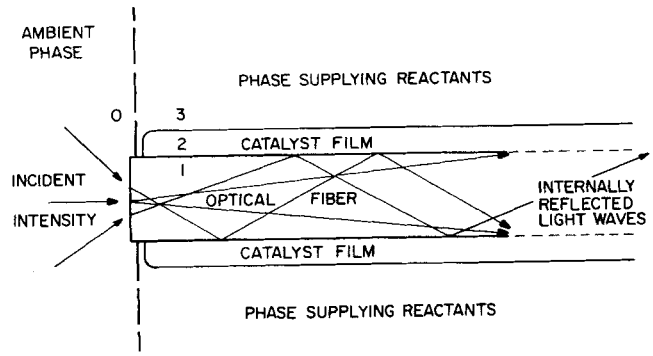

Fig. 2. Schematic drawing of the catalyst coated optical fiber concept.

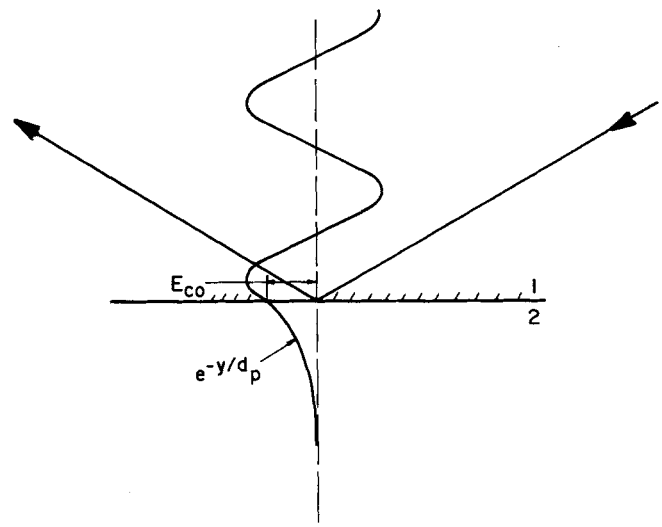

Fig. 3. Standing wave amplitude at a totally reflecting interface.

catalyst. The optical fiber might be considered to be a pore carrying the reactant, light, to the catalyst (Figure 2). The ratio of the cylindrical fiber surface to the circular fiber end surface (light entrance area) is $4L/d_f$. Since fiber lengths greater than 1 km and fiber diameters as small as 10 μm are produced commercially, evidently a very large catalyst area can be illuminated by light piped down the fiber from one end.

The piping effect, which establishes the utility of optical fibers as light wave guides in the communications industry, is based on the principle of internal reflection (Figure 3). When light in medium 1 strikes an interface between medium 1 and medium 2 at an angle θ to the surface normal, total internal reflection occurs if $n_1 > n_2$ and $\sin\theta > n_2/n_1$.* Although the light wave is reflected, the incoming and outgoing waves superimpose to form a standing wave in medium 1 which decays exponentially into the external medium 2 (Born and Wolf, 1965). The penetration of this *evanescent* wave is of the order of the wavelength of the light. Reflection is perfect if medium 2 is non-absorbing; a loss of reflected intensity occurs otherwise. This loss by an absorbing second medium is the basis for Internal Reflection Spectroscopy (IRS) (Harrick, 1967; Haller et al., 1976). Additional light losses can occur if the interface is rough (scattering)

* Typically, the index of refraction of semiconductors is greater than the index of refraction of glass in the nonabsorbing (long wavelength) region of the spectrum. In the absorbing (short wavelength) region, however, which is important for this application, the index of refraction for semiconductors such as titanium dioxide is less than that of glass ($n_1 > n_2$). Nevertheless, at the absorption edge ($h\nu$ = band gap energy), the index of refraction is very much greater than that of glass (infinite if the edge is sharp). Thus, a portion of the useful light may be internally reflected in the semiconductor layer ($n_2 > n_1$ and $n_3 > n_3$) (Cardona and Harbeke, 1965).

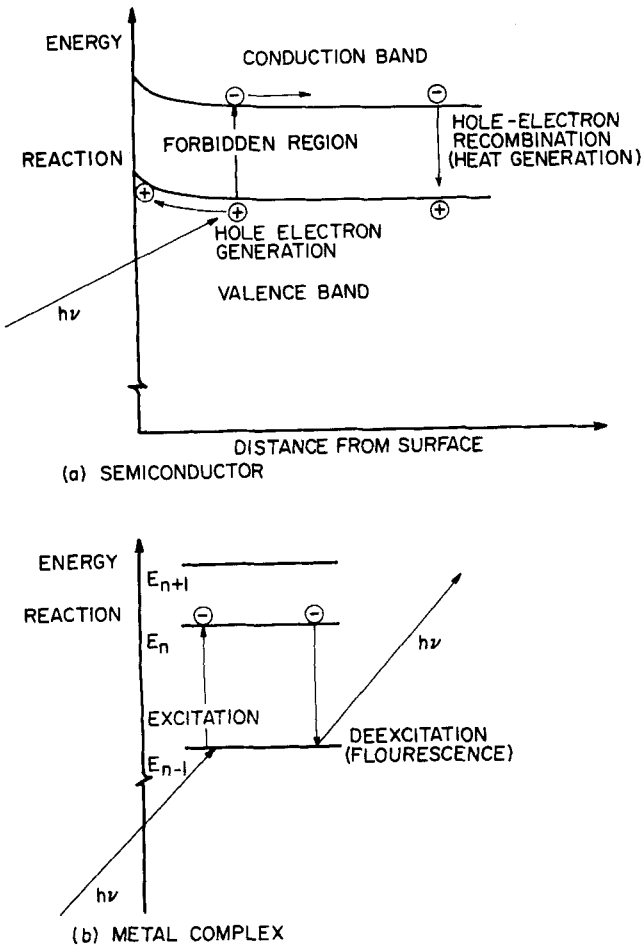

Fig. 4. Rates of excitation and deexcitation for (a) semiconductor and (b) metal complex.

or if absorption and scattering within the fiber occur due to impurities or bulk inhomogeneities (French, 1975).

These additional surface and bulk losses are very small for typical optical fibers. If an absorbing powder is at the reflecting surface, however, additional scattering losses may occur (Harrick, 1967). IRS, typically using a polished slab with parallel reflecting surfaces, has demonstrated that internal reflection can be used to contact repeatedly a large surface area of an absorbing phase, including either surfactant monolayers or powders (Harrick, 1967). Thus, the concept of the optical fiber coated with a heterogeneous absorber for photoassisted heterogeneous catalysis is based on experimental results which are reasonably described with internal reflection theories.

The apparent local heat of reaction ΔH_{app} consists of a term due to light absorbtion and a term due to chemical reaction (Marinangeli and Ollis, 1977). In gas-solid systems, such as the catalytic partial oxidation above, Prater numbers $[\equiv (-\Delta H_{app}) D_e A_o / k_e T_o]$ greater than unity may arise. Since the titanium dioxide activity drops for temperatures above 110°C, a large bulk gas/solid interface such as obtained by catalyst powder distribution over an optical fiber surface may aid catalyst temperature control and thus catalyst specific activity.

It is possible to saturate some photoassisted catalysts with relatively low light intensities. Saturation was observed for the D_2-H_2 reaction on magnesium oxide for intensities greater than 2×10^{-5} w/cm^2 (Harkins et al., 1969) and for titanium dioxide at high intensities (Wrighton et al., 1976*c*). Saturation occurs when the rate of photoexcitation to higher energy states in the catalyst is much greater than the sum of all rates of deactivation, including reaction (Figure 4). If catalyst saturation occurs, optical fibers could be used for distribution of concentrated light to larger catalyst surface areas.

Another potential advantage of distributing light within optical fibers is that the light does not pass through most of the reactant and product phases in the reactor. This may be advantageous when the product is generated as bubbles, as has been observed in the semiconductor electrolysis of water at moderate intensities (Ellis et al., 1976; Wrighton et al., 1976*a, b*). Since light is scattered and reflected at gas-liquid interfaces (such as bubbles), some of the incident radiation will be lost if it approaches the catalyst through the bulk liquid phase.

EXPERIMENTAL TECHNIQUES FOR FIBER-CATALYST ASSEMBLY

Technology for coating optical fibers with a porous, high-surface area, semiconducting layer already exists. In the soot deposition process for the production of high silica fibers (French, 1975; Keck and Schultz, 1973; Ikeda et al., 1974), the hydrolysis of silicon tetrachloride and titanium tetrachloride in a gas-oxygen flame produces a silica-titanium dioxide soot which is deposited on a silica rod. Similarly, the titanium dioxide catalyst particles for the catalytic partial oxidation of alkanes were prepared by the hydrolysis of anhydrous titanium tetrachloride in a hydrogen-oxygen diffusion flame. The particle diameter could be controlled between 6 and 150 nm by variation of the flame temperature and titanium tetrachloride flow rate (Caillet et al., 1959; Long and Teichner, 1965; Juillet et al., 1973; Formenti et al., 1972). Thus, deposition of titanium dioxide particles on optical fibers is clearly feasible. Van der Waals forces for particles of diameter less than 100 nm are sufficient to give permanent adherence (Davies, 1973); slight sintering to make the titanium dioxide layer continuous assures a permanent coating. For oxides of metals which do not have volatile halides, vaporization of the pure metal from a heated filament or an electron beam evaporation source followed by oxidation could be used (Bunshah and Raghuram, 1972).

A catalytic surfactant complex will obviously require a large surface area for production of substantial quantities of reaction products. The technology for coating fibers with surfactant monolayers dates from the Langmuir-Blodgett technique (Blodgett, 1935). Currently, monolayers of stearic acid, an 18 carbon surfactant, may be coated onto optical fibers which are formed into fiber bundles (Allan, 1973). Chlorophyll and the ruthenium complex are surface active owing to similar carbon chain is (Figure 1). In addition, IRS has been used to

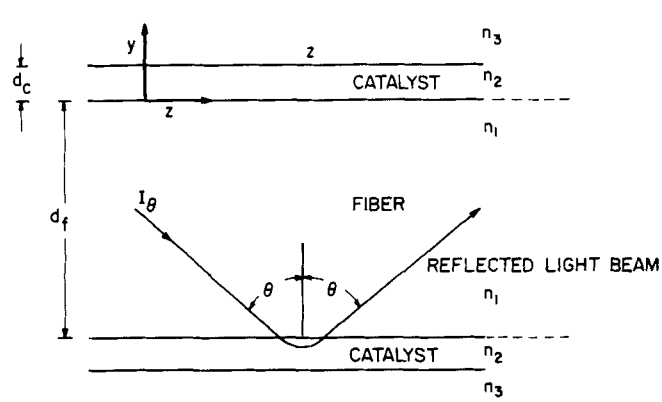

Fig. 5. Close-up of optical fiber showing pertinent variables and dimensions.

study absorbed monolayer and submonolayer quantities of stearic acid (Sharpe, 1961; Haller and Rice, 1970; Yang et al., 1974) and several fatty acids (Loeb, 1965), thus confirming the absorption of the piped light wave by adsorbed surfactant. Therefore, principles for making optical fibers coated with the surfactant catalytic complexes or more complicated multilayer assemblies are already evident, and the possibility of supplying light to an absorbing surfactant monolayer has been demonstrated.

Light transport analysis should reveal the important dimensionless group(s) and predict the axial (fiber) and radial (catalyst) light profiles. Three distinct cases arise corresponding to catalyst thicknesses d_c much less than, much greater than, or of the order of the light wavelength λ. A monolayer of surfactant gives $d_c \sim 2.5$ nm; thus, $d_c << \lambda \sim 400$ nm. With oxide semiconductors, development of the full space-charge region needed to retard electron-hole recombination (Hardee and Bard, 1975) might lead to $d_c >> \lambda$. Finally, semiconductors not needing a full space-charge region, or surfactant monolayers cast into multilayer assemblies, may lead to $d_c \sim \lambda$.

The physical geometry of the optical fiber suggests that the fiber may be considered to be analogous to a catalyst pore with reaction at the surface of the pore. The problem is then to analyze how the reactant, light, is transported through the pore and consumed in a cylindrical shell of active catalyst sites.

LIGHT TRANSFER AND CATALYST ABSORPTION: ISOLATED SINGLE FIBER

The photoassisted catalyzed rate will depend on the concentrations of reactants and on the light intensity in the catalyst film. In the following analysis, only an isolated, isothermal, single fiber will be considered. Subsequent papers consider various multiple fiber and nonisothermal situations, as well as electron (hole) transport.

The correct description of light transport arises from consideration of Maxwell's equations. Electromagnetic radiation of a large number of photons may be described by a transverse plane wave with associated electric and magnetic fields. The electric field vector $\vec{E}$ and the magnetic field vector $\vec{H}$ are orthogonal to each other and to the direction of the propagation; their amplitudes have a constant ratio $|\vec{E_o}/\vec{H_o}| = \sqrt{\mu/\epsilon}$. The intensity of an electromagnetic wave is given by the amplitude of the Poynting vector $|\vec{S_o}| = |(\vec{E}_x \times \vec{H})_o| = |\vec{E_o}||\sqrt{\epsilon/\mu}\,\vec{E_o}|$. The time average value of the Poynting vector equals the flow of electromagnetic energy. Since μ equals 1 for optical fibers and typical semiconductors, and the dielectric constant equals the square of the refractive index in medium i, n_i, then

$$I = n_i|\vec{E_o}|^2$$

To evaluate the intensity in the fiber and in the catalyst, a relationship between the electric field inside and outside the fiber is needed. Since the catalyst-fiber interface is exactly analogous to the sample (internal reflection element) interface for IRS, the approach of Harrick (Harrick, 1967) and others yielding this relationship applies. The analyses of thick, thin, and intermediate catalyst layers are developed from these principles in the following section.

Thin Films ($\lambda >> d_c$)

Consider an optical fiber of diameter d_f coated with a thin catalyst film of thickness d_c. Conservation of energy requires that over a cross section Δz long (Figure 5)

$$\text{Flux}|_{z+\Delta z} - \text{Flux}|_z + \text{Losses} = 0 \qquad (1)$$

The flux of light across the fiber cross section is

$$\text{Flux} = I_a \cdot \frac{\pi}{4} d_f^2 \qquad (2)$$

As a first approximation only, the loss due to the absorption of photons by the catalyst film will be considered. Losses due to impurity absorption in the fiber or wave scattering by defects at the film-fiber interface are included later.

In IRS or with a laser source, a single collimated light beam is used, whereas in applications using collected solar illumination or most artificial sources, light waves may arrive at the fiber-catalyst interface at angles varying from the critical angle for total reflection to 90 deg. A total absorption loss for the latter case can be determined by solving the single beam case and integrating over the appropriate angular distribution. Harrick's single-beam analysis involves an approximation that the absorption per reflection is small enough that the radial light intensity profile in the absence of absorption may be used in the local expression to calculate the absorption loss. He has determined that this approach is valid when the absorption per reflection is less than 10%. The absorption by a monolayer of the ruthenium complex on glass was 0.1 to 1.% (Sprintschnik et al., 1976).

The Lambert-Beer law may be used to determine the absorption loss in the monolayer:

$$dI_c = -\alpha_c I_c dy$$

For a small absorption and a thin catalytic film, it may be assumed that I_c is constant through the film at a particular value of z. Then

$$a = -\Delta I_c = \int_0^{d_c} \alpha_c I_c dy$$

$$a = \alpha_c I_c d_c \qquad (3)$$

The intensity of the beam in the catalyst film must be related to the axial intensity in the fiber. For a single interior beam striking the interface at an angle θ to the normal

$$I_\theta = n_1|\vec{E_{of}}|^2$$

The axial component of the intensity is

$$I_a = I_\theta \sin\theta$$

$$= n_1 \sin\theta|\vec{E_{of}}|^2 \qquad (4)$$

In the catalyst film

$$I_c = n_2|\vec{E_{oc}}|^2 \qquad (5)$$

Harrick has calculated the value of $|\vec{E_{oc}}|^2$ for a unit incident $\vec{E_{of}}$. The result depends on the polarization of the light as well as the indexes of refraction. Only isotropic absorption is considered below. (If the absorption is anisotropic, the losses for both parallel and perpendicular polarization can be developed leading to separate equations of identical form.)

For isotropic absorption

$$|\vec{E_{oc}}|^2 = |\vec{E}_{\parallel c}|^2 + |\vec{E}_{\perp c}|^2$$

$$|\vec{E_{oc}}|^2 = \frac{4\cos^2\theta}{(1-n_{31}^2)} + \frac{4\cos^2\theta[(1+n_{32}^4)\sin^2\theta - n_{31}^2]}{(1-n_{31}^2)[(1+n_{31}^2)\sin^2\theta - n_{31}^2]} \qquad (6)$$

Combining Equations (4) (5) and (6), we get

$$\frac{I_c}{I_a} = \frac{4n_{21}\cos^2\theta}{\sin\theta(1-n^2_{31})} \left[1 + \frac{(1+n^4_{32})\sin^2\theta - n^2_{31}}{(1+n^2_{31})\sin^2\theta - n^2_{31}}\right] \equiv \beta_c \quad (7)$$

where $\beta_c = f(n_1, n_2, n_3, \theta)$. The result of these definitions is

$$a = \alpha_c \beta_c I_a d_c$$

The differential loss is the amount absorbed per fiber surface area a multiplied by $(\pi d_f \Delta z)$:

$$\text{Loss} = \alpha_c \beta_c I_a d_c d_f \pi \Delta z$$

Substitution into Equation (1) yields as $\Delta z \to 0$

$$\frac{\pi d_f^2}{4}\frac{dI_a}{dz} + \alpha_c \beta_c d_c d_f \pi I_a = 0 \quad (8)$$

Defining

$$\xi = z/L, \quad \psi = I/I_o, \quad \text{and} \quad \phi = \frac{4\alpha_c \beta_c d_c L}{d_f}$$

we get the dimensionless form of (8):

$$\frac{d\psi_a}{d\xi} + \phi\psi_a = 0 \quad (9)$$

The group ϕ is the ratio of the maximum absorption rate per reflection $\alpha_c \beta_c d_c I_o$ to the available absorption rate per reflection $I_o/(L/d_f)$. The ratio, which may be called the Harrick number, is similar to the Thiele modulus which relates the maximum rate of reactant consumption to the available rate of reactant supply. With

$$\psi_a(0) = 1$$

the solution for (9) is

$$\psi_a = \exp(-\phi\xi) \quad (10)$$

Photoassisted heterogeneously catalyzed reactions are typically first order in incident intensity, provided that deexcitation is fast relative to absorption (saturation does not occur). For such a first-order dependency, an effectiveness factor is defined as the ratio of the average value of the intensity in the catalyst film to the intensity in the film without light transport limitations:

$$\eta = \frac{\overline{I_c}}{I_{co}} = \frac{\overline{I_c}}{\beta_c I_o}$$

In dimensionless terms

$$\eta = \psi_c/\beta_c = \overline{\psi_a}$$

For a fiber of length L

$$\overline{\psi_a} = \int_0^1 \psi_a(\xi)\,d\xi$$

$$\eta = \frac{1}{\phi}[1 - \exp(-\phi)] \quad (11)$$

For $\phi << 1$

$$\exp(-\phi) \simeq 1 - \phi$$

Thus, for $(\phi << 1)$

$$\eta \simeq \frac{1}{\phi}[1 - (1-\phi)] \simeq 1$$

For $(\phi >> 1)$, $\exp(-\phi) \simeq 0$, so

$$\eta \simeq \frac{1}{\phi}$$

An effectiveness factor can be obtained for reactions which are n^{th} order in intensity (ϕ is replaced by $n\phi$). The first law of photochemistry (Calvert and Pitts, 1966) states that the fundamental step in a photochemical reaction requires one photon. Since it is conceivable that a series of steps involving successive promotions of excited species could occur, the n^{th} order effectiveness factor is given by

$$\eta = \frac{1}{n\phi}[1 - \exp(-n\phi)] \quad (n > 1) \quad (12)$$

The same limiting form arises as saturation is approached $(n < 1)$. In the limit as $n \to 0$ (saturation), $\eta \to 1$ again. For monochromatic illumination with an angular distribution of intensity, the initial intensity at $z = 0$ will be $I_o R(\theta)$, where $R(\theta)$ is a normalized distribution function

$$\int_\theta R(\theta)\,d\theta = 1$$

Then, the initial condition is

$$\psi_a(0) = R(\theta)$$

Since $\beta_c = \beta_c(\theta)$ and ϕ depends on β_c, then

$$\psi_a(\theta, \xi) = R(\theta)\exp[\xi\phi(\theta)]$$

The total intensity profile is then given by

$$\psi_a(\xi) = \int_{\theta_c}^{\pi/2} R(\theta)\exp[-\xi\phi(\theta)]\,d\theta$$

since the range of possible angles of incidence is θ_c to $\pi/2$ [where the critical angle is defined by $\theta_c = \sin^{-1}(n_2/n_1)$].

For polychromatic radiation, the possible wavelength dependence of the absorption coefficient may be included. In this general case, $\phi = \phi(\theta, \lambda)$. If the initial normalized distribution of intensity vs. wavelength and angle is $R(\lambda, \theta)$, then

$$\psi_a(\theta, \lambda, \xi) = R(\theta, \lambda)\exp[-\xi\phi(\theta, \lambda)] \quad (13)$$

The total intensity profile is given by

$$\psi_a(\xi) = \int_{\theta_c}^{\pi/2}\int_{\lambda_{min}}^{\lambda_{max}} R(\theta, \lambda)\exp[-\xi\phi(\theta, \lambda)]\,d\lambda\,d\theta \quad (14)$$

The effectiveness factor is

$$\eta = \int_{\theta_c}^{\pi/2}\int_{\lambda_{min}}^{\lambda_{max}} R(\theta, \lambda)\frac{1}{n\phi(\theta, \lambda)}\{1 - \exp[-n\phi(\theta, \lambda)]\}\,d\lambda\,d\theta \quad (15)$$

Thin Films ($d_c >> \lambda$)

In a thick film, the radial decline of intensity in the catalyst film must be included. Harrick's approach (Harrick, 1967) may again be used. In the alkane oxidation studies (Formenti et al., 1971), a thickness of 10 to 15 μm of titanium dioxide powder reduced direct incident illumination to a negligible level. With internal reflection, the predominant catalyst illumination arises from the evanescent (not scattered) wave which penetrates to only the order of 0.4 μm. Thus, the absorption is expected to be less than 10% in this region.

The loss in the film is

$$a = -\int dI_c = \int \alpha_c I_c\,dy$$

$$I_c = n_2|\vec{E}_c|^2$$

The electric field of the evanescent wave decreases exponentially in the absence of absorption (Born and Wolf, 1965):

$$\vec{E}_c = \vec{E}_{oc} e^{-y/d_p} \tag{16}$$

$$d_p = \frac{\lambda_1}{2\pi(\sin^2\theta - n^2_{21})^{1/2}} \tag{17}$$

Since Harrick's approximation of small absorption per reflection is being used, the decrease in the electric field due to absorption locally by the catalyst can be neglected, but the radial decay term in (16) remains.

The decrease in intensity due to the increasing cylindrical area through the annular catalyst film is negligible if $d_p << d_f$. As d_p is of the order of λ (say 400 nm), this approximation is good for commercially available optical fibers (diameters 10 to 1 000 μm). (If the wavelength is of the order of the fiber diameter, the transport of light is similar to transport in hollow conductors; only certain modes are permitted.)

Placing (16) into the expression for the absorption, we get

$$a = \int_o^\infty \alpha_c n_2 |\vec{E}_{oc}|^2 e^{-2y/d_p} dy$$

$$a = \frac{\alpha_c n_2 |\vec{E}_{oc}|^2 d_p}{2}$$

$$a = \frac{\alpha_c I_{oc} d_p}{2}$$

As in the thin film case, I_{oc}, the intensity in the film at the interface, must be related to the axial flux by the relationship

$$I_{oc} = \beta_c' I_a$$

The interface relationships are (4) and (5):

$$I_a = n_1 \sin\theta \, |\vec{E}_{of}|^2$$

$$I_c = n_2 |\vec{E}_{oc}|^2$$

For a unit electric field incident at angle θ, Harrick has calculated $|\vec{E}_{oc}|^2$ in the presence of a thick film for a unit incident $\vec{E}_f$:

$$|\vec{E}_{oc}|^2 = |\vec{E}_\perp|^2 + |E_\parallel|^2$$

$$|\vec{E}_{oc}|^2 = \frac{4\cos^2\theta}{(1 - n^2_{21})}\left[1 + \frac{2\sin^2\theta - n^2_{21}}{(1 + n^2_{21})\sin^2\theta - n^2_{21}}\right] \tag{18}$$

A combination of Equations (4), (5), and (18) gives

$$\beta_c' = \frac{4\cos^2\theta \, n_{21}}{\sin\theta(1 - n^2_{21})}\left[1 + \frac{2\sin^2\theta - n^2_{21}}{(1 + n^2_{21})\sin^2\theta - n^2_{21}}\right] \tag{19}$$

As a result, the loss over a differential interfacial area, $\pi d_f \Delta z$, is

$$\text{Loss} = \alpha_c \beta_c' d_p I_a d_f \pi \Delta z/2$$

With this expression, the equation for the loss of light in the fiber becomes

$$\frac{d\psi_a}{d\xi} + \phi'\psi_a = 0 \tag{20}$$

with ψ_a and ξ as before, and

$$\phi' = \frac{2\alpha_c \beta_c' d_p L}{d_f} \tag{21}$$

Integration with $\psi_a(0) = 1$ gives the dimensionless intensity in the fiber:

$$\psi_a = \exp(-\phi'\xi) \tag{22}$$

The dimensionless intensity in the catalyst film is

$$\psi_c = \beta_c' \psi_a e^{-2\gamma} \tag{23}$$

$$\gamma = \frac{y}{d_p}$$

Thus, the complete expression for the dimensionless intensity in the film is

$$\psi_c = \beta_c' \exp[-\phi'\xi - 2\gamma] \tag{24}$$

The average value of ψ_c at ξ is

$$\overline{\psi}_c(\xi) = \frac{\int_0^\infty \psi_c d\gamma}{d_c}$$

(Since $\gamma_{\max} \equiv d_c/d_p >> 1$, the integration is taken from 0 to ∞ for convenience)

$$\overline{\psi}_c(\xi) = \frac{\beta_c' \exp(-\phi'\xi)}{2d_c} \tag{25}$$

A reaction effectiveness factor is defined as for the thin film case:

$$\eta = \frac{\int_0^1 [\psi_c(\xi)]^n d\xi}{[\psi_c(0)]^n}$$

$$\eta = \frac{1}{n\phi'}[1 - \exp(-n\phi)] \tag{26}$$

A more general effectiveness factor must be derived when mass or heat transfer limitations also intrude. This may occur in thick catalyst layers; the problem is considered in a second paper (Marinangeli and Ollis, 1977).

As in the thin film case, the possible angular distribution of intensity and wavelength dependence may be included:

$$\psi_a = (\theta, \lambda, \xi) = R(\theta, \lambda)\exp[-\xi\phi'(\theta, \lambda)] \tag{27}$$

$$\psi_a(\xi) = \int_{\theta_o}^{\pi/2} \int_{\lambda_{\min}}^{\lambda_{\max}} R(\theta, \lambda)\exp[-\xi\phi'(\theta, \lambda)] \tag{28}$$

$$\psi_c(\xi, \gamma) = \beta_c' \psi_a(\xi)\exp[-2\gamma] \tag{29}$$

The effectiveness factor is

$$\eta = \frac{\int_{\theta_o}^{\pi/2} \int_{\lambda_{\min}}^{\lambda_{\max}} R(\theta, \lambda)\beta_c' \frac{1}{n\phi'}\{1 - \exp[n\phi'(\theta, \lambda)]\} d\theta d\lambda}{\int_{\theta_o}^{\pi/2} \beta_c' d\theta} \tag{30}$$

Intermediate Film Thickness

This analysis is similar to the thick film case, with two differences. When the absorption in Δz is calculated, the integration is from 0 to d_c, the catalyst film thickness:

$$a = \int_0^{d_o} \alpha_c n_2 |\vec{E}_{oc}|^2 e^{-2y/d_p} dy$$

In addition, the relationship between the incident intensity in the film and the intensity in the catalyst changes:

$$I_{oc} = \beta_c'' I_a$$

A value of β_c'' can be determined for an intermediate

film thickness by applying the formulas of Hansen (Hansen, 1968). These formulas are relatively complicated and are not reproduced here; they are suitable for digital computation. As a result of these changes, the Harrick number becomes

$$\phi'' = \frac{2\alpha_c\beta_c'' d_p L}{d_f}\left[1 - \exp\left(-\frac{2d_c}{d_p}\right)\right] \quad (31)$$

where the axial light intensity is given by

$$\frac{d\psi_a}{d\xi} + \phi''\psi_a = 0 \quad (32)$$

The same solutions for ψ_c and η result as for the thick film case:

$$\psi_c = \beta_c'' \exp(-\phi''\xi - 2\gamma)$$

where now $0 \leq \gamma \leq d_c/d_p \equiv \gamma_{\max}$. Equation (30) gives the general effectiveness factor.

Impurity Absorption and Scattering

In optical communications, absorption at the interface is avoided by coating the fiber with a nonabsorbing dielectric. The only losses are due to scattering by bulk inhomogeneities, absorption by impurities in the fiber, and scattering losses due to imperfections at the interface. For a reflecting beam traveling through the fiber, these internal losses may be expressed as (Allan, 1973)

$$I_\theta/I_o = \exp\left[\frac{-L}{\sin\theta}\left(\alpha_f + \beta_f\frac{\cos\theta}{d_f}\right)\right]$$

The loss due to bulk absorption and scattering depends exponentially on α_f, the fiber absorption coefficient, multiplied by the beam path length $L/\sin\theta$. The loss due to scattering at the wall is related to β_f, an intrinsic surface loss per reflection, multiplied by the number of times the beam strikes the wall in a length L, $(L/d_f)\cot\theta$. In differential form

$$\frac{dI_a}{dx} + \left(\frac{\alpha_f}{\sin\theta} + \frac{\beta_f\cot\theta}{d_f}\right)I_a = 0$$

Thus, the equation including intrinsic losses and catalyst absorption is

$$\frac{d\psi_a}{d\xi} + \left(\phi + \frac{\alpha_f L}{\sin\theta} + \frac{\beta_f L\cot\theta}{d_f}\right)\psi_a = 0 \quad (33)$$

A new dimensionless group may be defined:

$$\Phi = \left(\phi + \frac{\alpha_f L}{\sin\theta} + \frac{\beta_f L\cot\theta}{d_f}\right) \quad (34)$$

Clearly, this group is a function of θ, and possibly λ. If this group replaces ϕ (or ϕ' or ϕ'') in Equations (9), (20), or (32), the analyses for the light profiles in the fiber remain the same.

An additional term must be added to include a scattered (as well as evanescent) wave in the catalyst:

$$\psi_{oc} = \beta_c\psi_a + \frac{(\beta_f L n_{21}\cot\theta)}{d_f}\psi_a$$

Thus, the light intensity in the catalyst is the sum of the evanescent wave contribution and the scattered wave contribution (almost all of which does not return to the fiber). The two contributions decay exponentially but with different characteristic depths; that is

$$\psi_{ce} = \beta_c\psi_a e^{-2\gamma}$$

for the evanescent wave and

$$\psi_{cs} = \frac{\beta_f L n_{21}\cot\theta}{d_f}\psi_a e^{-\alpha_c y}$$

for the scattered wave with Lambert-Beer absorption. Defining

$$\delta = \alpha_c y \quad (35)$$

$$\tau = \beta_f L n_{21}\cot\theta/d_f \quad (36)$$

we get

$$\psi_{cs} = \tau\psi_a e^{-\delta}$$

The final expressions for the dimensionless intensity of light at any point in the catalyst is

$$\psi_c = \psi_a(\beta_c e^{-2\gamma} + \tau e^{-\delta}) \quad (37)$$

$$\psi_a = e^{-\Phi\xi} \quad (38)$$

Of course, these expressions can be integrated over appropriate angular or wavelength distributions for polychromatic light incident at many different angles.

In general, the value for α_f is so small that it will be negligible for this case (Allan, 1973). It is much more difficult to judge a priori the relative magnitude of β_f. Dust particles (French, 1975) and trapped air bubbles (Tynes et al., 1971) at fiber optic interfaces enhance scattering losses. The effect of surface irregularities increases as the fiber diameter decreases; the scattering losses increase almost as $1/(d_f)^2$ (Tynes et al., 1971). Pitted depressions smaller than several hundred angstroms in diameter or depth do not exert a significant reflection loss, though (Allan, 1973). For bulk scattering by irregularities much smaller than the wavelengths, Rayleigh scattering predominates. When bulk irregularities are much larger than the wavelength, forward Mie scattering predominates (French et al., 1975; Ostermayer and Benson, 1974). Unfortunately, the open literature does not described the variation in β_f with the size of the interfacial disturbance. It is evident, however, that the size of catalyst particles and of the coated fiber itself ought to determine the scattering loss. Thus, control of the catalyst particle size, as may be accomplished with the soot deposition technique, offers an opportunity to increase the intensity of light supplied to a less absorbing catalyst and to supply light to catalyst particles located outside the evanescent field.

Entrance Effects

A brief consideration of geometric optics will relate the intensity and angular distribution of light incident on the collecting end of an optical fiber to the initial internal intensity and angular distribution (Allan, 1973). A beam (in a less dense medium) incident at angle ω on the fiber end will be split into a refracted beam, which enters the fiber, and a reflected beam as shown in Figure 6. From Snell's law

$$n_o\sin\omega = n_1\sin\omega'$$

$$n_o\sin\omega = n_1\cos\theta$$

Therefore

$$\omega = \sin^{-1}\left(\frac{n_1}{n_o}\cos\theta\right) \quad (39)$$

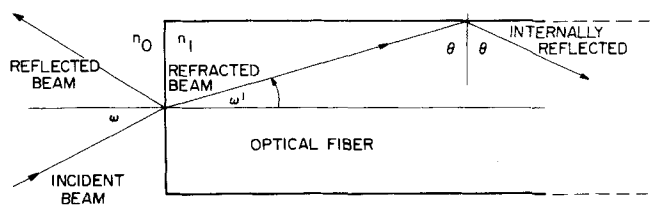

Fig. 6. Passage of a meridional light ray into an optical fiber.

or

$$\theta = \cos^{-1}\left(\frac{n_o}{n_1}\sin\omega\right) \tag{40}$$

Equations (39) and (40) provide the relationship between internal and external beam angles.

The relationship between the incident and transmitted intensities for a beam impinging at an angle ω are given by the Fresnel formulas (Born and Wolf, 1965). The Fresnel transmissivity differs for parallel and perpendicular polarization:

$$I_{\omega_\perp}{}' = T_\perp I_{\omega_\perp}$$

$$I_{\omega''}{}' = T_{''} I_{\omega''}$$

$$T_\perp = \frac{\sin 2\omega \sin 2\omega'}{\sin^2(\omega+\omega')} \tag{41}$$

$$T_{''} = \frac{\sin 2\omega \sin z\omega'}{\sin^2(\omega+\omega')\cos^2(\omega-\omega')} \tag{42}$$

If the polarization of the incident light is known, these equations may be used to determine the Fresnel loss

$$I_{\omega'}/I_\omega = \frac{T_\perp I_{\omega_\perp} + T_{''} I_{\omega''}}{I_{\omega_\perp} + I_{\omega''}} = T^* \tag{43}$$

When the polarization of the light is not known, the approximation below may be adequate for small angles, ω (Born and Wolf, 1965)

$$T^* = 4n/(n+1)^2$$

For a given external light distribution

$$I(\omega) = I_i S(\omega)$$

the internal distribution $I_o R(\theta)$ is given by

$$I(\theta) = T^*(\omega) I_i R(\omega)$$

$$\omega = \sin^{-1}\left(\frac{n_1}{n_o}\cos\theta\right)$$

The fiber will capture a fraction of light which is incident within a core defined by a critical capture angle:

$$\omega_c = \sin^{-1}\left(\frac{n_1}{n_o}\cos\theta_c\right)$$

Light incident at angles greater than ω_c will enter the fiber but will not be totally reflected at the fiber wall, that is, will not be well piped down the fiber.

Part of the incident light cannot be captured owing to the reflection loss and the restriction that $\omega < \omega_c$. The capture cone is centered on $\omega = 0$; the Fresnel reflection loss is also minimized for $\omega = 0$. Fortunately, the intensity of the incident light will often peak at $\omega = 0$. For instance, diffuse light which is incident on a fiber end which is perpendicular to the fiber axis has a distribution

$$I(\omega) = I_i \cos\omega$$

The optical fiber will capture a fraction of this light equal to

$$I/I_{\text{Total}} = \int_o^{\omega_c} T^*(\omega)\cos(\omega)\, d\omega$$

For typical parameters $n_o = 1$, $n_1 = 1.5$, and $n_2 = 1.3$, with diffuse light centered at $\omega = 0$, the fiber will capture 63% of the incident light. For directed light incident at $\omega = 0$, the fiber captures 94% of the incident light. Thus, a fiber can capture most diffuse light as well as most direct light within a critical angle ω_c. (An additional loss arises in bundled fibers due to space between fibers.)

For any particular incident light distribution, such as from a solar collector, the preceding equations can be used to determine the fraction of light collected

$$I/I_{\text{Total}} = \int_o^{\omega_c} T^*(\omega) R(\omega)\, d\omega \tag{44}$$

$$\omega_c = \sin^{-1}\left(\frac{n_1}{n_o}\cos\theta_c\right) \tag{45}$$

and the internal angular intensity distributions:

$$I(\theta) = T^*(\omega) I_i R(\omega) \tag{46}$$

$$\omega = \sin^{-1}\left(\frac{n_1}{n_o}\cos\theta\right) \tag{47}$$

Partially Reflected Rays

The preceding discussions have considered only totally internally reflected light beams. Light which strikes the fiber-catalyst interface at $\theta < \theta_c$ will be partially transmitted; the remainder will be internally reflected down the fiber. The proportions of transmitted and reflected light depend on the Fresnel transmissivity [Equations (41) and (42)]. For perpendicular polarization, the fraction of partially reflected light remaining in the fiber at an axial distance z from the fiber end is

$$I_\perp/I_{o_\perp} = (1 - T_\perp)^{z/d_f \tan\theta}$$

For parallel polarization

$$I_{''}/I_{o''} = (1 - T_{''})^{z/d_f \tan\theta}$$

These ratios are the fractions of light reflected per encounter with the interface, raised to the power of the number of reflections.

The contributions of the transmitted light to the intensity in the concentric catalyst layer are

$$I_{c_\perp} = I_\perp T_\perp \exp(-\alpha_c y)$$

$$I_{c''} = I_{''} T_{''} \exp(-\alpha_c y)$$

or

$$I_{c_\perp} = I_{o_\perp} T_\perp (1 - T_\perp)^{z/d_f \tan\theta} \exp(-\alpha_c y) \tag{48}$$

$$I_{c''} = I_{o''} T_{''} (1 - T_{''})^{z/d_f \tan\theta} \exp(-\alpha_c y) \tag{49}$$

The Effect of Fiber Curvature

It is possible to flex optical fibers. This will be useful if it is desirable to confine a long fiber (or fiber bundle) to a limited space by coiling the fiber. Obviously, the incident angle between a light beam and the normal to the fiber-catalyst interface will change. The consequences of bending optical fibers have been considered previously (Allen, 1973).

If a meridional ray enters a curved section of optical fiber with a radius of curvature R at a distance from the axis of $\Delta, (-d_f/2 \leq \Delta \leq d_f/2)$, the relationships between the angle of incidence in the straight fiber θ_o and the angle of incidence for the external interface θ_1 and for the internal interface θ_2 are (Allen, 1973)

$$\sin\theta_2 = \frac{R + (d_f/2)}{R - (d_f/2)}\sin\theta_1 \tag{50}$$

$$\sin\theta_2 = \frac{R + \Delta}{R - (d_f/2)}\sin\theta_o \tag{51}$$

From these equations, it follows that

$$\theta_2 \geqq \theta_o \geqq \theta_1$$

Thus, a ray which is internally reflected in a straight

fiber may escape at the outer surface of a coiled fiber for a sufficiently small radius of curvature. When R is smaller than (Allen, 1973)

$$R = \frac{\Delta \sin\theta_o + (d_f/2)}{1 - \sin\theta_o}$$

the reflected ray does not strike the internal interface at all.

The path length for a reflected beam is decreased by bending the fiber. The ratio of path lengths between rays in curved and straight fibers is (Allen, 1973)

$$L^*/L = \frac{R^2 - (d_f^2/4)}{R^2 + R\Delta} \frac{\sin(\theta_2 - \theta_1)}{\theta_2 - \theta_1} \qquad (52)$$

In addition, the number of reflections per length may change. The number of reflections per unit length in a straight fiber is

$$N = \frac{1}{d_f \tan\theta_o}$$

In a curved fiber

$$N^* = \frac{1}{d_f \tan\theta_1 + \frac{(\theta_2 - \theta_1) d_f}{2}} \qquad (53)$$

Of course, the effectiveness factor for a curved fiber will change. The value of β, the ratio of the intensity in the catalyst to the intensity in the fiber, is a function of the angle of incidence. Clearly, β will vary with the polar angle about the fiber axis, and an average value can be calculated.

ACKNOWLEDGMENT

This study was supported by the National Science Foundation and the Energy Research and Development Administration.

NOTATION

a = absorption loss per area $= -\Delta I$
A_o = reactant concentration
d_c = catalyst thickness
d_f = fiber diameter
d_p = depth of penetration of the evanescent wave
D_e = effective diffusivity of reactant A in the catalyst
$\vec{E}_o$ = electric field amplitude
$\vec{E}$ = electric field vector
$\vec{E}_c$ = electric field vector in the catalyst
$\vec{E}_{\parallel c}$ = parallel component of electric field vector in the catalyst
$\vec{E}_{\perp c}$ = perpendicular component of electric field vector in the catalyst
$\vec{E}_f$ = electric field vector in the fiber
$\vec{E}_{oc}$ = electric field vector at the interface in the catalyst
$\vec{E}_{of}$ = electric field vector at the interface in the fiber
$\vec{H}$ = magnetic field vector
$\vec{H}_o$ = magnetic field amplitude
ΔH_{app} = apparent enthalpy of reaction
ΔH_f = enthalpy of formation
I = light intensity
I_a = axial light intensity
I_i = incident light intensity
I_o = initial light intensity in the fiber
I_{co} = light intensity in the catalyst at the fiber-catalyst boundary
R = radius of curvature of curved fiber
I_θ = light intensity of an internal beam incident at θ
I_ω = light intensity of an external beam incident at ω
k_e = effective thermal conductivity of catalyst layer
L = fiber length
n = reaction order
n_i = index of refraction in medium 1
n_{ij} = n_i/n_j
n_o = ambient index of refraction
n_1 = fiber index of refraction
n_2 = catalyst index of refraction
n_3 = outermost phase index of refraction
$R(\lambda)$ = normalized wavelength distribution
$R(\theta, \lambda)$ = normalized internal angular and wavelength distribution
$S(\omega)$ = normalized external angular distribution
T_o = ambient temperature
$T_\parallel$ = Fresnel transmissivity for parallel polarization
$T_\perp$ = Fresnel transmissivity for perpendicular polarization
T^* = total transmissivity
y = radial coordinate into catalyst from the interface
z = axial coordinate
$\vec{S}$ = Poynting vector

Greek Letters

α = absorption coefficient
α_c = absorption coefficient of catalyst
α_f = absorption coefficient of fiber
β_c = ratio of I_{co}/I_a for the thin film case
β_c' = ratio of I_{co}/I_a for the thick film case
β_c'' = ratio of I_{co}/I_a for the intermediate film thickness case
β_f = intrinsic surface loss per reflection
γ = dimensionless distance into the catalyst from the interface (characteristic for the evanescent wave) $= y/d_p$
Δ = distance between the axis of the fiber and the point of entry of a beam into a curved section of fiber
δ = dimensionless distance into the catalyst from the interface (characteristic for the scattered wave) $= \alpha_c r$
ϵ = dielectric constant
η = effectiveness factor
θ = angle between reflecting beam and normal to the interface
θ_c = critical angle for reflection
λ = light wavelength
μ = magnetic permeability
ν = frequency of light
ξ = dimensionless axial distance (z/L)
τ = $\beta_f L n_{21}/d_f$
ϕ = $\dfrac{4\alpha_c\beta_c d_c L}{d_f}$
ϕ' = $\dfrac{2\alpha_c\beta_c' d_c L}{d_f}$
ϕ'' = $\dfrac{2\alpha_c\beta_c'' d_c L}{d_f}\left[1 - \exp\left(\dfrac{-2d_c}{d_p}\right)\right]$
Φ = $(\phi + \alpha_f L/\sin\theta + \beta_f L \cot\theta/d_f)$ or $(\phi' + \alpha_f L/\sin\theta + \beta_f L \cot\theta/d_f)$ or $(\phi'' + \alpha_f L/\sin\theta + \beta_f L \cot\theta/d_f)$
ψ = dimensionless light intensity
ψ_a = axial dimensionless light intensity
ψ_c = dimensionless light intensity in the catalyst

ψ_{ce} = evanescent contribution to ψ_c
ψ_{cs} = scattered contribution to ψ_c
ω = angle between the light beam incident on the end of the fiber and the fiber axis (meridional ray)
ω' = angle between the light beam refracted into the fiber and the fiber axis (meridional ray)

Superscripts

$'$ = thick film
$''$ = intermediate film
$\rightarrow$ = vector
$*$ = bent fiber

Subscripts

a = axial
c = catalyst
e = evanescent
f = fiber
o = related to ambient phase or initial property
p = penetration
s = scattered
1 = fiber phase
2 = catalyst phase
3 = medium suppling reactants
$\perp$ = perpendicular polarization
$''$ = parallel polarization

LITERATURE CITED

Allan, W. B., *Fiber Optics: Theory and Practice,* Plenum Press, New York (1973).

Blodgett, K. B., "Films Built by Depositing Successive Monomolecular Layers on a Solid Surface," *J. Am. Chem. Soc.,* **57,** 1007 (1935).

Born, M., and E. Wolf, *Principles of Optics,* 3 ed., Pergamon Press, Oxford, England (1965).

Bunshah, R. F. and A. C. Raghuram, "Activated Reactive Evaporation Process for High Rate Deposition of Compounds," *J. Vac. Sci. Technol.,* **9,** 1385 (1972).

Caillat, R., J. P. Cuer, J. Elston, F. Juillet, R. Pointud, M. Prettre, and S. J. Teichner, "Preparation of Homodispersed Oxides in the Oxygen-Hydrogen Flame and Properties of the Compounds," *Bull. Soc. Chim. France,* 152 (1959).

Calvert, J. G., and J. N. Pitts, Jr., *Photochemistry,* J. Wiley, New York (1966).

Cardona, M., and G. Harbeke, "Optical Properties of Wurtzite-Type Crystals and Rutile," *Phys. Rev.,* **137,** A1467 (1965).

Cassano, A. E., P. L. Silveston, and J. M. Smith, "Photochemical Reactor Engineering," *Ind. Eng. Chem.,* **59,** 18 (1967).

Cerdà, J., H. A. Irazoqui, and A. E. Cassano, "Radiation Fields Inside an Elliptical Photoreflector with a Source of Finite Spatial Dimensions," *AIChE J.,* **19,** 963 (1973).

Davies, C. N., *Air Filtration,* Academic Press, New York (1973)

Djeghri, N., M. Formenti, and F. Juillet, "Photointeraction of the Surface of Titanium Dioxide between Oxygen and Alkanes," *Chem. Soc. London, Faraday Disc.,* **58,** 185 (1974)

Dolan, W. J., C. A. Dimon, and J. S. Dranoff, "Dimensional Analysis in Photochemical Reactor Design," *AIChE J.,* **11,** 1000 (1969).

Ellis, A. B., S. W. Kaiser, and M. S. Wrighton, "Semiconducting Potassium Tantalate Electrodes. Photoassistance Agents for The Efficient Electrolysis of H_2O," *J. Phys. Chem.,* **80,** 1325 (1976).

Formenti, M., F. Juillet, P. Meriaudeau, and S. J. Teichner, "Heterogeneous Photocatalysis for Partial Oxidation of Paraffins," *Chem. Technol.,* **1,** 680 (1971).

———, and P. Vergnon, "Preparation in a Hydrogen-Oxygen Flame of Ultrafine Metal Oxide Particles. Oxidative Properties Toward Hydrocarbons in the Presence of Ultraviolet Radiation," *J. Coll. Interface Sci.,* **39,** 79 (1972).

Formenti, M., P. Meriaudeau, F. Juillet, and S. J. Teichner, "Heterogeneous Photocatalysis. Partial and Total Oxidation of Hydrocarbons and Inorganic Compounds at Room Temperature on Solid Catalyst under Irradiation," *Fifth International Congress on Catalysis,* Palm Beach, North Holland Publishing, Amsterdam 1011 (1973).

Formenti, M. F. Juillet, and S. J. Teichner, "Systematic Study of the Heterogeneous Photocatalytic Oxidation of Hydrocarbons," Compte Rendu de fin de contrat d'une recherche financeé par la Délégation générale à la recherche scientifique et technique, Contrat No. 73 7 13 19 (1974).

French, W. G., J. B. MacChesney, and A. D. Pearson, "Glass Fibers for Optical Communications," *Ann. Rev. Materials Sci.* **5,** 373 (1975).

French, W. G., *Materials for Fiber Optics Communications,* Bell Laboratories, Murray Hill, N.J. (Oct., 1975).

Freund, T., and W. P. Gomes, "Electrochemical Methods for Investigating Catalysis by Semiconductors," *Catalysis Rev.,* **3,** 1(1969).

Fujishima, A., and K. Honda, "Electrochemical Photolysis of Water at a Semiconductor Electrode," *Nature,* **238,** 37 (1972).

Hacker, D. S., and J. B. Butt, "Photocatalysis in a Slurry Reactor," *Chem. Engrg. Sci.,* **30,** 1149 (1975).

Haller, G. L., and R. W. Rice, "A Study of the Adsorption on Single Crystals by IRS," *J. Phys. Chem.,* **74,** 4386 (1970).

———, and C. Z. Wan, "Applications of Internal Reflection Spectroscopy to Surface Studies," *Catalysis Rev.,* **13,** 259 (1976).

Hansen, W. N., "Expended Formulas for Attenuated Total Reflection and the Deviation of Absorption Rules for Single and Multiple ATR Spectrometer Cells," Spectrochimica Acta, **21,** 815 (1965).

Hansen, W. N., "Electric Fields Produced by the Propagation of Plane Coherent Electromagnetic Radiation in a Stratified Medium," *J. Opt. Soc. Am.,* **58,** 380 (1968).

Harano, Y., and T. Matsura, "Problems in Designing Photochemical Reactors," *Intern. Chem. Eng.,* **12,** 131 (1972).

Hardee, K. L., and A. J. Bard, "Semiconductor Electrodes. I. The Chemical Vapor Deposition and Application of Polycrystalline N-type TiO_2 Electrodes to the Photosensitized Electrolysis of H_2O," *J. Electrochem. Soc.,* **122,** 739 (1975).

Harkins, C. G., W. W. Shang, and T. W. Leland, Relation of the Catalytic Activity of MgO to its Electron Energy States," *J. Phys. Chem.,* **73,** 130 (1969).

Harrick, N. J., *Internal Reflection Spectroscopy,* Interscience Publishers, New York, (1967).

Ikeda, Y., M. Yoshiyagawa, and Y. Furuse, "Low Loss Glasses for Light-Focusing Fiber Waveguides," *Ninth International Congress Glass* **6,** 82 (1974).

Irazoqui, H. A., J. Cerdá, and A. E. Cassandro, "Radiation Profiles in an Empty Annular Photoreactor with a Source of Finite Spatial Dimensions," *AIChE J.,* **19,** 460 (1973).

Jacob, S. M., and J. S. Dranoff, "Light Intensity Profiles in an Elliptical Photoreactor," *AIChE J.,* **15,** 141 (1969).

———, "Light Intensity Profiles in a Perfectly Mixed Photoreactor," *ibid.,* **16,** 359 (1970).

Juillet, F., F. Lecompte, H. Mozzanega, S. J. Teichner, A. Thevenet, and P. Vergnon, "Inorganic Oxide Aerosols of Controlled Submicronic Dimensions," *Farraday Symposia of the Chemical Society,* **7,** 57 (1973).

Keck, D. B., and P. C. Schultz, "Method of Forming Optical Waveguide Fibers," *U.S. Patent 3,711,262* (1973).

Loeb, G., Private communication quoted in Harrick, *Internal Reflection Spectroscopy,* page 269 (1965).

Long, J., and S. J. Teichner, "Preparation of TiO_2 in the Oxygen-Hydrogen Flame to Homodispersed Spherical Particles," *Rev. Hautes Temp. Refractories,* **2,** 47 (1965).

Markham, M. C. and K. J. Laidler, "A Kinetic Study of Photooxidation on the Surface of Zinc Oxide in Aqueous Suspensions," *J. Phys. Chem.,* **57,** 363 (1953).

Marinangeli, R. E., and D. F. Ollis, "Photoassisted Catalysis with Optical Fibers. II. Transport Influences in the Fiber Bundle," to be submitted to *AIChE J.* (1977).

Matsuura, T., and J. M. Smith, "Light Distribution in Cylindrical Photoreactors," *AIChE J.,* **16,** 321 (1970).

Murphy, W. R., T. F. Veerkamp, and T. W. Leland, "Effect of Ultraviolet Radiation on Zinc Oxide Catalysts," *J. Catalysis,* **43,** 304 (1976).

Ostermayer, F. W. Jr., and W. W. Benson, "Integrating Sphere for Measuring Scattering Loss in Optical Fiber Waveguides," *Appl. Optics,* **13,** 1900 (1974).

Paleocrassas, S., "Photolysis of Water as a Solar Energy Conversion Process: An Assessment," *Hydrogen Energy*, p. 243 (Hydrogen Economy, Miami Energy Conference, Miami Beach, Fla., 1974).
Rabl, A., V. J. Sevcik, R. M. Guigler, and R. Winston, "Use of Compound Parabolic Concentrator for Solar Energy Use," Progress Report for July-December, 1974, Argonne National Lab-75-42 (1974).
Roger, M., and J. Villermaux, "Light Distribution in Cylindrical Photoreactors," *AIChE J.*, **21**, 1207 (1975).
Sharpe, L. H., "Observation of Molecular Interactions in Oriented Monolayers by Infrared Spectroscopy Involving Total Internal Reflection," *Proc. Chem. Soc.*, **1961**, 461 (1961).
Sprintschnik, G., H. W. Sprintschnik, P. P. Kirsch, and D. G. Whitten, "Photochemical Cleavage of Water: A System for Solar Energy Conversion Using Monolayer-Bound Transition Metal Complexes," *J. Am. Chem. Soc.*, **98**, 2337 (1976).
Takahashi, F. and R. Kituchi, "Photoelectrolysis Using Chlorophyll Electrodes," *Biochim. Biophys. Acta.*, **430**, 490 (1976).
—— "Preparation and Photochemical Reactivity of Surfactant Ruthenium (II) Complexes in Monolayer Assemblies and at Water-Solid Interfaces," private communication from D. O. Whitten, (1977).
Tynes, A. R., A. D. Pearson, and D. L. Bisbee, "Loss Mechanisms and Measurements in Clad Glass Fibers and Bulk Glass," *J. Opt. Soc. Am.*, **61**, 143 (1971).
Wolkenstein, Th., "The Electronic Theory of Photocatalytic Reactions on Semiconductors," *Advances in Catalysis*, **23**, 157 (1973).
Wrighton, M. S., D. S. Ginley, P. T. Wolczanski, A. B. Ellis, D. L. Morse, and A. Linz, "Photoassisted Electrolysis of Water by Irradiation of a Titanium Dioxide Electrode," *Proc. Natl. Acad. Sci. USA*, **72**, 1518 (1975).
Wrighton, M. S., D. L. Morse, A. B. Ellis, D. S. Ginley, and H. B. Abrahamson, "Photoassisted Electrolysis of Water by Ultraviolet Irradiation of an Antimony Doped Stannic Oxide Electrode," *J. Am. Chem. Soc.*, **98**, 44 (1976*a*).
Wrighton, M. S., A. B. Ellis, P. T. Wolczanski, D. L. Morse, H. B. Abrahamson, and D. S. Ginley, "Strontium Titanate Photoelectrodes: Efficient Photoassisted Electrolysis of Water at Zero Applied Potential," *ibid.*, 2774 (1976*b*).
Wrighton, M. S., J. M. Bolts, A. B. Ellis, and S. W. Kaiser, "Photoassisted Electrolysis of Water: Conversion of Optical to Chemical Energy," Proc. 11th Intersociety Energy Conversion Eng. Conf., 1, 35 (Sept. 12-17, 1976*c*).
Yang, R. T., J. B. Fenn, and G. L. Haller, "Surface Diffusion of Stearic Acid on Aluminum Oxide," *AIChE J.*, **20**, 735 (1974).
Zolner, W. J. III., and J. A. Williams, "Three Dimensional Light Intensity Distribution Model for an Elliptical Photoreactor," *ibid.*, **17**, 502 (1971).

Manuscript received December 13, 1976 and accepted February 22, 1977.

Vertical Distribution of Dilute Suspensions in Turbulent Pipe Flow

A. J. KARABELAS

Westhollow Research Center
Shell Development Company
Houston, Texas 77001

Closed-form expressions are presented for predicting vertical concentration distribution of the dispersed phase in the turbulent core of pipe and channel flow. Experimental data obtained with spherical particles, of mean diameter d_{50} comparable to the Kolmogorov microscale, are in good agreement with model predictions. The average value of dimensionless lateral particle diffusivity, $\zeta = \epsilon/Ru_*$, determined from these data is approximately 0.25, that is, fairly close to previously reported measurements with much coarser particles.

SCOPE

In steady horizontal pipe flow, the density difference between a dispersed solid or liquid phase and the continuous fluid phase can cause a nonuniform distribution of the dispersion in the pipe cross section. From a theoretical point of view, an accurate method for calculating particle or droplet concentration distribution can be very helpful in modeling dispersed two-phase flow systems. From a practical standpoint, prediction of flow conditions associated with large concentration gradients is often desirable, for example, in the design and operation of transfer lines in process units and of long distance pipelines transporting slurries. The particular problem motivating the present work is the development of flow criteria for a sufficiently uniform distribution of sediment and water in crude oil pipelines which are necessary for capturing a representative sample.

A simple diffusion type of model, proposed many years ago (O'Brien, 1933; Rouse, 1937) for vertical sediment distribution in open channels and rivers is usually applied to steady flow in closed conduits as well. This model, however, has some serious limitations, especially in the case of relatively concentrated suspensions of a wide size spectrum. Hunt (1954, 1969) has presented a more complete description of solids distribution in turbulent flow and has applied it to open channel flow. The main objective of this study was to use Hunt's formulation for pipe flow and to develop a general expression, predicting concentra-